American Mineralogist, Volume 76, pages 1683–1693, 1991

Ba-rich micas from the Franklin Marble, Lime Crest and Sterling Hill, New Jersey

Robert J. Tracy
Department of Geological Sciences, Virginia Polytechnic Institute and State University, Blacksburg, Virginia 24061, U.S.A.

Abstract

Compositionally unusual Ba-rich micas have been found in the Franklin Marble at the Lime Crest quarry and at Sterling Hill, both in New Jersey. At Lime Crest, coarse calcite-dolomite marble is cut by very small veins containing green and colorless micas, albite, fluorite, pyrite, and chromian rutile. Large green muscovite flakes are superficially similar to comparable barian and chromian muscovite from Isua and Malene, West Greenland: BaO contents range up to 12 wt% (about ⅓ of the A site), and Cr_2O_3 contents, though typically about 1 wt%, can be as high as 4 wt%. Smaller muscovite grains in recrystallized marble on vein margins have the lowest Ba and highest Cr contents. Barian, fluorian phlogopite, also on vein margins, has about 3 wt% of both BaO and F and very low total Fe. Formation of these Ba-, Cr-, and F-rich minerals is clearly related to vein formation, and vein-forming fluids were presumably the transport agents for the elements that are not typically concentrated in the marble.

At Sterling Hill, Ba-rich biotite has been found in an augite-willemite-gahnite-sphalerite-calcite skarn. This biotite is bright orange in plane-polarized light and contains from 4 up to about 25 wt% BaO. Changes in concentration of a number of other elements are correlated with Ba content. The micas highest in Ba are also high in total Fe and in Fe/Mg ratio, and qualify to be called anandite. They differ spectacularly from previously reported anandite, however, in having about 7 wt% Cl, and they are by far the most Cl-rich micas yet described. The Ba-rich micas also are higher than low-Ba micas in content of NiO (0.24 vs. 0.10 wt%) and MnO (2.3 vs. 1.7 wt%) but lower in content of ZnO (4–5 vs. 8–9 wt%) and TiO_2 (0.7 vs. 1.5–2 wt%). Although the whole barian mica compositional range can be seen in a single thin section, there is no textural evidence to indicate chronology of formation. A scenario has been constructed in which isochemical metamorphism of the skarn protolith resulted in formation of Ba-rich sheet silicates and sphalerite as a result of thermal breakdown and reduction of hydrothermal barite in the presence of hydrothermal Zn- and Mn-rich ore minerals, minor admixed detrital sediments, and pore fluids. Rapid depletion of the small reservoirs of Ba, Fe, and Cl apparently resulted in subsequent formation of biotite much poorer in Ba, Cl, and Fe. These micas appear to have survived a granulite-grade metamorphic peak, although they may have been reconstituted during cooling.

Introduction

The replacement of univalent alkali metal cations (typically K^{1+}) by divalent alkaline earth cations in the interlayer cation sites of the micas is a well-known phenomenon. The substitution must of course also involve a coupled charge reduction in other sites, accomplished most commonly by replacing $^{[4]}Si$ with $^{[4]}Al$, sometimes referred to as the "plagioclase substitution" and expressed as the exchange vector $Ca^{A}\,{}^{[4]}Al(Na,K)_{-1}Si_{-1}$. The typical replacement is by Ca, which yields the dioctahedral mica end-member margarite [$CaAl_4Si_2O_{10}(OH)_2$] and the trioctahedral mica clintonite [$CaMg_2Al_3Si_2O_{10}(OH)_2$]. Superimposed upon these end-members can be other mica-group substitutions such as the Tschermak and Ti-Tschermak exchanges and the replacement of OH^{-1} by F^{-1} or Cl^{-1}.

The significant substitution of Ba into the interlayer sites of muscovite is quite rare but has been reported from several metamorphic environments, as reviewed by Guggenheim (1984). "Oellacherite" is an obsolete name that was applied in the 19th century to Ba-bearing muscovite (typically with up to 20% of the interlayer site occupied by Ba), and pink barian muscovite was reported from Franklin, New Jersey, by Bauer and Berman (1933) and further studied by Dunn (1984). Dymek et al. (1983) reported green muscovite with Ba and Cr from Isua, West Greenland, that has similar Ba and Cr contents to that from the Frankin Marble reported in this paper. I have not found other reports of barian muscovite.

On the other hand, there are more numerous reports and analyses of barian biotite from both igneous and metamorphic occurrences. Igneous occurrences of barian, titanian phlogopite have been reported from an alkaline

0003–004X/91/0910–1683$02.00

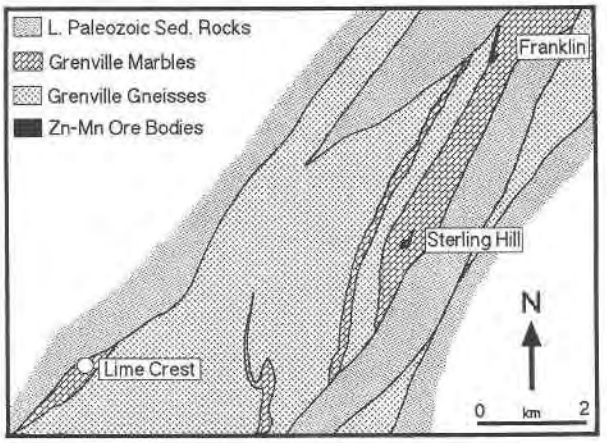

Fig. 1. Geologic sketch map of the Franklin–Sterling Hill–Lime Crest area in Sussex County, northern New Jersey.

ultramafic plug in Montana (Wendlandt, 1977), nephelinite from Oahu (Mansker et al., 1979), and Brazilian carbonatite (Gaspar and Wyllie, 1982). Yoshii et al. (1973) described and named the new metamorphic mineral kinoshitalite, a barian, manganoan analogue of phlogopite. Solie and Su (1987) described a low-Mn, kinoshitalite-like mineral from the Middle Fork plutonic complex, Alaska. Both of these metamorphic barian biotite occurrences are in calc-silicates or marbles. Other metamorphic calc-silicate occurrences include barian phlogopite in marble from Rogaland, Norway (Bol et al., 1989), and Ba,Mn phlogopite in ore skarn from Långban, Sweden (Frondel and Ito, 1968). Ba- and Fe-rich mica, called anandite, has been reported from the type locality, Wilagedera, Sri Lanka (Pattiaratchi et al., 1967), as well as from several other skarn localities cited by Guggenheim (1984). The barian micas reported in the present paper span a range in composition from barian phlogopite to anandite.

In this paper, I present data on two barium mica occurrences (Fig. 1): bright green barian, chromian muscovite and barian, fluorian phlogopite from a vein in the Franklin Marble in the Lime Crest quarry and micas with a wide range of Ba contents from skarn interlayered with ore in the Sterling Hill mine. The Franklin Marble is a Grenville-age calcite-dolomite marble in New Jersey and adjacent New York. Much of the unit is rather monotonous, coarse-grained marble, but locally it contains a remarkable array of minerals. Well over 300 oxide and silicate minerals, 33 not known to occur anywhere else, have been reported from the famous zinc ore deposits at Franklin and Sterling Hill (see the excellent summary in Frondel and Baum, 1974). The nature of the protoliths of the ore deposits has been debated extensively for almost 150 years, but a new study (Johnson, 1990) argues persuasively for their origin as deep-sea hydrothermal brine deposits consisting of oxides, hydroxides, and hydroxysilicates of Zn and Mn. The ore minerals and associated calc-silicates and skarns apparently formed as a result of granulite-grade metamorphism (Carvalho and Sclar, 1988). At both ore deposits and at the Lime Crest quarry about 6 miles away, pegmatite dikes have intruded the coarse marble and created a variety of contact metasomatic mineral occurrences.

The occurrence of Ba-rich biotite in the skarn at the Sterling Hill mine and barian muscovite and fluorian phlogopite in veins at Lime Crest is problematic in the sense that no definite source for the Ba has yet been found in the vicinity. However, Ba-bearing minerals, including barite, barian feldspars, and barian micas, have long been known from the Franklin Furnace and Sterling Hill mines (Frondel and Baum, 1974). There are no reported barite-bearing evaporite horizons in the Precambrian stratigraphic section in northern New Jersey, which includes abundant felsic and minor mafic gneisses as well as marble, although such evaporites have been reported in Grenville rocks near the sulfide ores at Balmat-Edwards, New York (Lea and Dill, 1968). At Lime Crest, Ba has presumably been mobilized from an unidentified local source, perhaps an evaporite, and transported by metamorphic fluids. There are hints in the chemistry of the micas themselves as to the nature of these fluids, as will be discussed. At Sterling Hill, in the absence of evidence for synmetamorphic Ba metasomatism, a case can be made for isochemical metamorphism of a protolith in which original hydrothermal minerals, including barite, were metamorphosed to form the present-day assemblage.

Barian, chromian micas at Lime Crest

Petrography and mineral chemistry

The Lime Crest quarry is in an isolated lens of coarse marble about 2 miles west of the main belt of Franklin Marble. On the northeast side of the quarry, near the main access road to the quarry floor, several thin greenish veins in coarse marble were exposed in the quarry wall in 1983, when the samples were collected. In hand specimen, the veins were only a few millimeters wide and contained megascopic bright emerald green mica flakes, pale purple fluorite cubes, tan albite grains up to several millimeters across, and pyrite crystals up to 0.5 cm. In thin section, the veins can be seen to consist mainly of pale green muscovite and somewhat altered albite, with large euhedral crystals up to 5 mm long of Cr-rich rutile. The coarse calcite-dolomite marble is significantly recrystallized on the borders of the veins and contains isolated small flakes of fluorian phlogopite and of green barian, chromian muscovite that have compositions quite different from the larger muscovite crystals in the veins.

Mineral analyses reported in this paper were all done on ARL SEMQ and Cameca SX-50 electron microprobes at VPI and SU. Operating conditions were 15-kV accelerating potential and 15-nA sample current on brass. Standards included Amelia albite (Na,Al,Si), rutile (Ti), fayalite (Fe), norbergite (Mg,F), Benson orthoclase (K), barian apatite (Ba,Cl), rhodonite (Mn), and Durango apatite (Ca). Raw data were corrected using ZAF correc-

tions (Heinrich, 1981). Operating conditions were appropriate for the unknowns, based on analyses of internal standards, including micas.

Representative microprobe analyses of phlogopite and muscovite from the marble are given in Table 1. The table reports three representative analyses each of barian, fluorian phlogopite and barian, chromian muscovite; both minerals show unusual chemistry. First, note the significantly high Ba content of both minerals, with roughly 8–10% of the interlayer site occupied by Ba. Also note that up to 20% of the interlayer site in phlogopite is occupied by Na, unusually high for biotite. The Cr_2O_3 content of the muscovite is also high, up to 3.5 wt%, and explains its deep green color. Finally, the F content of the phlogopite is high at about 3 wt%, or about 30–35% fluorian phlogopite end-member. However, F contents this high are not unusual for phlogopite in Grenville marbles, which can approach being fluorian end-members (Valley et al., 1982).

Examination of the muscovite structural formulas in Table 1 indicates an unusual combination of crystal-chemical substitutions. Very high MgO contents, along with normal FeO, are reflected as substantial phengite substitution (approximately 30%), characterized by the exchange vector $(Mg,Fe)SiAl_{-2}$. However, the silica content in excess of 3.0 does not balance the octahedral R^{2+} content because of simultaneous operation of a silica-reducing vector: $BaAlK_{-1}Si_{-1}$. In addition to the additive component $KAl_3Si_3O_{10}(OH)_2$, there are seven nonnegligible exchange vector components required to describe the muscovite composition space: (1) NaK_{-1}, (2) $BaAlK_{-1}Si_{-1}$, (3) $CaAlK_{-1}Si_{-1}$, (4) $(Fe,Mg)SiAl_{-2}$, (5) $CrAl_{-1}$, (6) $TiAlAl_{-1}Si_{-1}$, and (7) $F(OH)_{-1}$; components 2, 4, and 5 dominate.

In addition to the small disseminated mica flakes described above, there are larger green muscovite grains up to several millimeters in size associated with albite and chromian rutile in the veins. These larger grains are strongly zoned, with cores enriched in Ba, Na, and Cr relative to the rims and K enriched in rims. Table 2 gives representative analyses from a probe traverse of a single muscovite crystal; analysis 1 is from the rim and 9 is from the core. Ba is substantially higher and Cr is lower in these muscovite samples than in those described above, but they are also megascopically green in color. Although the analyses given in Table 2 come from a grain that is smoothly and symmetrically zoned, BSE and X-ray imaging of a number of grains has disclosed abrupt compositional changes, commonly in the form of thin, sharply bounded bands of K-richer muscovite parallel to (001). Data on K, Ba, Na, and Cr from one probe traverse are shown as a function of distance across the grain in Figure 2, and these are used in succeeding plots. Note the crudely symmetrical form of the zoning in Figure 2 and the magnitude of change in the alkalis and in Ba. Implications of this chemistry for the origin of the micas will be discussed below.

The composition space occupied by Lime Crest muscovite can be illustrated using a variety of two-dimensional subspace diagrams. The first of these, Figure 3, shows the interlayer cation populations of the muscovite along with the barian biotite from Lime Crest and Sterling Hill. Most of the muscovite data shown in Figure 3 are from the zoned crystal traverse, and the rest were obtained from isolated flakes of high-Cr muscovite such as those from Table 1. Note that all the Lime Crest micas, both muscovite and phlogopite, fall on a rough trend of proportional decrease of Ba and Na (in a constant ratio of about 50:50) with increase in K. This suggests growth of micas in the marble from an unchanging reservoir of Ba and Na without progressive fractionation of these elements. The direction of zoning in the muscovite, from (Ba,Na)-rich cores to K-rich rims, further suggests depletion of this reservoir accompanied by progressively greater incorporation of K into the micas. The role of the veins in altering the composition of the marble locally is likely to be crucial here and will be assessed in a later section.

Because Ba shows significant variation within these micas, it is important to assess the relationships of other components to changes in Ba. An obvious correlation should be the $^{[4]}Al$ content as a function of alkaline earth content (Ba + Ca) according to exchanges 2 and 3. Figure 4 illustrates this relationship for two data sets, one from the zoned crystal (A) and the other from isolated flakes (B). Both sets of data reflect the expected, approximately

TABLE 1. Electron microprobe analyses of barian, fluorian phlogopite and barian, chromian muscovite from the Lime Crest quarry

	1	2	3	4	5	6
SiO_2	39.03	37.86	38.25	44.45	44.32	44.36
TiO_2	0.41	0.47	0.44	0.31	0.25	0.49
Al_2O_3	16.98	17.22	16.90	29.24	28.97	30.44
Cr_2O_3	0.76	0.80	0.79	3.24	3.51	2.22
FeO	0.80	1.45	0.79	0.50	0.45	0.36
MnO	0.05	0.05	0.02	0.02	0.03	0.02
MgO	24.75	23.73	25.12	2.75	2.78	2.53
CaO	0.13	0.12	0.08	0.22	0.23	0.20
BaO	2.88	3.18	3.22	2.42	2.79	2.81
Na_2O	1.17	0.49	1.34	0.36	0.41	0.44
K_2O	7.42	8.96	7.34	9.62	9.61	9.43
F	2.87	3.30	2.86	0.32	0.34	0.32
Total	97.25	97.63	97.15	93.45	93.69	93.62
$-O = F$	1.21	1.39	1.20	0.13	0.14	0.13
Total	96.04	96.24	95.95	93.32	93.55	93.49
	Formulas on 11 O atom anhydrous basis					
Si	2.781	2.737	2.741	3.107	3.105	3.090
Al	1.219	1.263	1.259	0.893	0.895	0.910
	4.000	4.000	4.000	4.000	4.000	4.000
Al	0.207	0.231	0.168	1.516	1.497	1.589
Ti	0.022	0.023	0.023	0.016	0.013	0.026
Cr	0.043	0.045	0.045	0.179	0.194	0.122
Fe	0.047	0.088	0.048	0.029	0.027	0.021
Mn	0.003	0.003	0.002	0.001	0.002	0.001
Mg	2.628	2.557	2.684	0.286	0.291	0.263
	2.950	2.947	2.970	2.027	2.024	2.022
Ca	0.010	0.009	0.006	0.017	0.017	0.015
Ba	0.080	0.090	0.090	0.066	0.076	0.076
Na	0.161	0.069	0.187	0.050	0.056	0.060
K	0.674	0.826	0.670	0.858	0.859	0.838
	0.925	0.994	0.953	0.991	1.008	0.989
F	0.646	0.754	0.649	0.072	0.074	0.070

TABLE 2. Representative electron microprobe analyses from a traverse of a single zoned barian, chromian muscovite sample from the Lime Crest quarry

	1	2	3	4	5	6	7	8	9
SiO_2	43.08	42.99	41.71	40.73	40.32	39.99	39.19	38.36	38.62
TiO_2	0.32	0.21	0.24	0.39	0.22	0.36	0.45	0.53	0.58
Al_2O_3	37.06	37.45	37.78	38.41	37.85	38.01	38.14	37.62	37.47
Cr_2O_3	0.54	0.74	0.75	0.62	0.87	0.90	0.88	1.10	1.05
FeO	0.15	0.12	0.10	0.10	0.12	0.12	0.11	0.13	0.14
MnO	0.03	0.03	0.04	0.03	0.02	0.04	0.03	0.04	0.04
MgO	0.91	0.86	0.58	0.44	0.67	0.72	0.66	0.76	0.67
CaO	0.26	0.06	0.06	0.08	0.08	0.07	0.08	0.10	0.09
BaO	4.79	5.61	6.58	7.59	8.01	8.95	9.45	10.82	11.41
Na_2O	1.23	1.66	2.09	2.36	2.16	2.16	2.25	2.19	1.74
K_2O	7.17	6.01	5.39	4.64	5.04	4.46	3.94	3.69	3.98
F	0.20	0.17	0.13	0.12	0.14	0.11	0.14	0.15	0.11
Total	95.74	95.91	95.45	95.51	95.50	95.89	95.32	95.49	95.90
$-O = F$	0.08	0.07	0.06	0.05	0.06	0.05	0.06	0.06	0.05
Total	95.66	95.84	95.39	95.46	95.44	95.84	95.26	95.43	95.85
				Formulas on 11 O atom anhydrous basis					
Si	2.919	2.910	2.857	2.803	2.796	2.774	2.743	2.714	2.729
Al	1.081	1.090	1.143	1.197	1.204	1.226	1.257	1.286	1.271
	4.000	4.000	4.000	4.000	4.000	4.000	4.000	4.000	4.000
Al	1.879	1.898	1.907	1.919	1.889	1.881	1.890	1.851	1.849
Ti	0.017	0.011	0.012	0.020	0.012	0.019	0.023	0.028	0.031
Cr	0.029	0.039	0.040	0.034	0.048	0.049	0.049	0.061	0.058
Fe	0.008	0.007	0.006	0.006	0.007	0.007	0.007	0.007	0.008
Mn	0.002	0.002	0.002	0.002	0.001	0.002	0.002	0.002	0.002
Mg	0.092	0.087	0.060	0.046	0.069	0.075	0.068	0.080	0.070
	2.027	2.044	2.027	2.027	2.026	2.033	2.039	2.029	2.018
Ca	0.019	0.004	0.005	0.006	0.006	0.005	0.006	0.008	0.007
Ba	0.127	0.149	0.177	0.205	0.218	0.243	0.259	0.300	0.316
Na	0.162	0.218	0.278	0.314	0.291	0.291	0.305	0.300	0.238
K	0.620	0.519	0.471	0.407	0.446	0.395	0.351	0.333	0.359
	0.928	0.890	0.931	0.932	0.961	0.934	0.921	0.941	0.920
F	0.042	0.037	0.028	0.026	0.030	0.024	0.032	0.034	0.025

linear, increase of $^{[4]}$Al with (Ba + Ca), but they obviously lie on lines with different intercepts. Least-squares fits indicate intercepts of 0.94 for the A data and 0.76 for the B data, although this latter intercept is not well constrained because of the limited data range. The intercepts in both cases closely predict the mean phengite content within each data set, calculated as percent phengite = $\{1.0 - [^{[4]}\text{Al} - (\text{Ba} + \text{Ca}) - \text{Ti}]\} \times 100$.

Other correlations with Ba are shown in Figure 5, which contains plots first used by Dymek et al. (1983). Figure 5

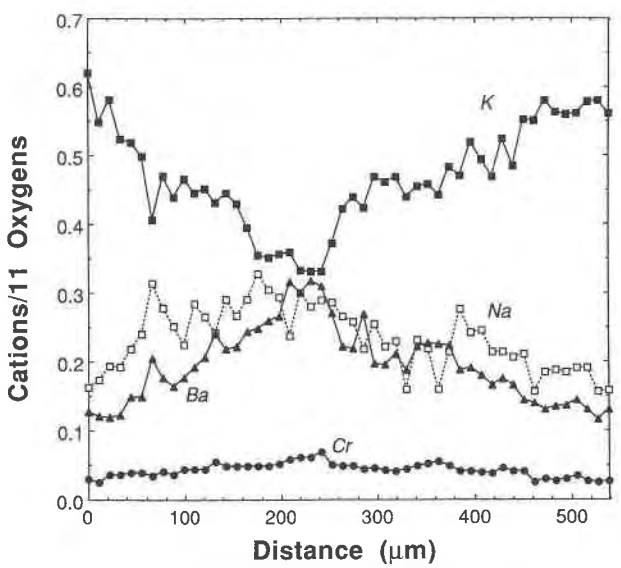

Fig. 2. Edge-to-edge zoning profile for K, Ba, Na, and Cr across a zoned green muscovite grain from the vein at Lime Crest. Note the strongly sympathetic behavior of Ba and Na. Although the zoning is crudely symmetrical, coupled shifts such as those between 60 and 80 μm may indicate thin lamellae of either high- or low-Ba mica (see text).

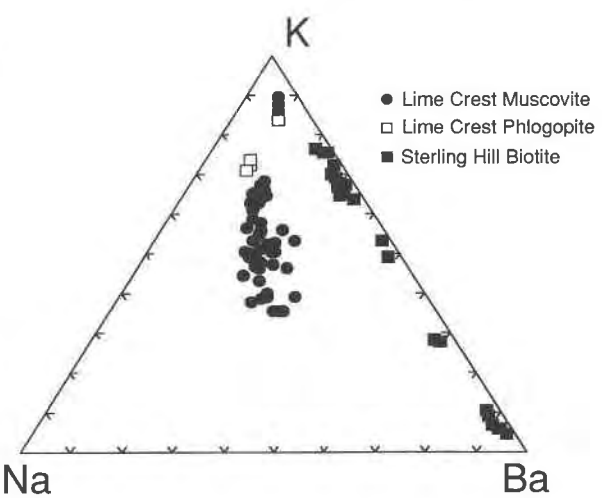

Fig. 3. Ternary K-Ba-Na plot showing the interlayer site compositions of all the micas discussed in this paper. Note the roughly constant Ba/Na ratio (about 1:1) in the micas from Lime Crest, regardless of K content.

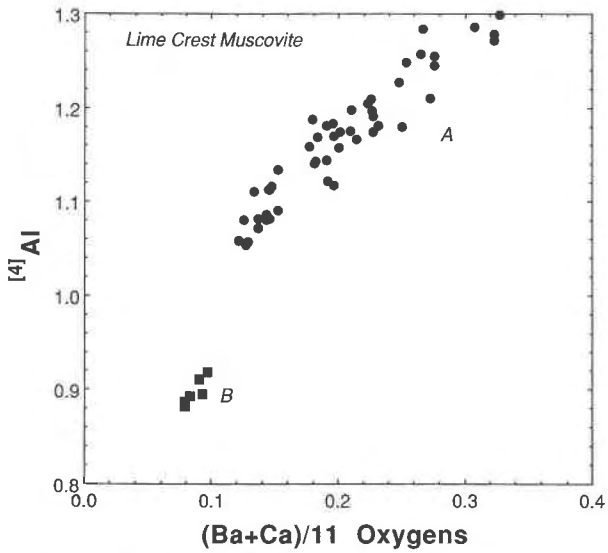

Fig. 4. Correlation of [4]Al with (Ba + Ca)/11 O atoms to illustrate the margarite-type substitution mechanism. Data A are from large zoned green muscovite grains in the vein, whereas data B are from the small muscovite grains in the vein periphery. Note the deficiency in [4]Al for data B, signifying a greater phengite content for these muscovite samples. Intercepts of least-squares fits on the *Y* axis indicate phengite content (see text): intercept for A is 0.94, and for B it is 0.76.

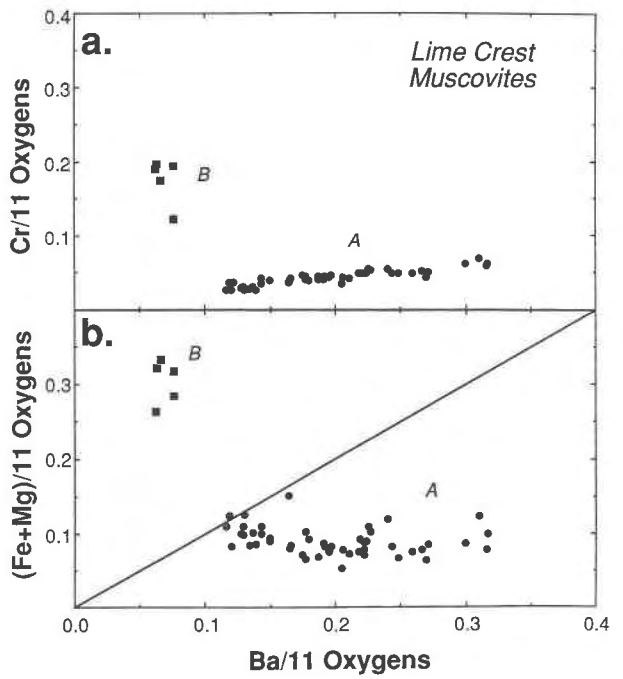

Fig. 5. (a) Correlation of Ba with Cr for Lime Crest muscovite, after a plot suggested by Dymek et al. (1983), emphasizing the chemical contrast between data sets A and B (see caption for Fig. 4). These data are superficially similar to those for the Malene green micas (Dymek et al., 1983) but differ in having much lower Cr contents. (b) Correlation of Ba and (Fe + Mg), after a plot from Dymek et al. (1983). Virtually all the compositions from the zoned grain show (Fe + Mg) < Ba, similar to B2 muscovite from Malene. The Lime Crest B data (see Fig. 3) are most similar to Malene type A green micas.

shows a quite linear sympathetic relationship between Ba and Cr for data set A, from the zoned crystal, whereas data set B shows much higher Cr contents with low Ba contents. Although these data are superficially similar to those of Dymek et al. (1983), the micas from Greenland have substantially higher Cr contents, up to extreme values of 1.0 Cr/11 O atoms, with intermediate Ba contents. The New Jersey muscovite has higher maximum Ba contents, however, and also shows relatively high Cr with low Ba in data set B. Figure 5 allows another comparison of the New Jersey muscovite with that from Greenland: data set A has (Fe + Mg) < Ba, similar to B_2 muscovite from Malene, whereas data set B is most like type A Malene green micas. None of the New Jersey muscovite seems to resemble the green micas from Isua.

Origin of barian, chromian micas at Lime Crest

Dymek et al. (1983) noted that the association of Ba and Cr is not common and explained the Ba-Cr enrichments of the Archean Malene and Isua green micas as a function of sedimentary or tectonic mixing of barite-bearing chemical sediments with clastic materials containing detrital chromite. They cited work by Devaraju and Anantha (1978) on interlayering of fuchsite schists and barite deposits in Archean rocks of India as support of this mechanism for mixing the two elements. These appear to be the only two reports of Ba-Cr occurrences in the literature, and they vary in two important ways from the Franklin Marble occurrence. The first and most obvious is that both earlier reported occurrences are in Archean rocks, whereas the Franklin Marble is Proterozoic. Its protolith age is actually indeterminate, although probably less than 2.0 Ga, but its Grenville metamorphism is well constrained at about 1050 Ma. Second, the other Ba-Cr occurrences are in fine-grained clastic rocks, dominantly green quartzites with subordinate gneisses and schists (Dymek et al., 1983), whereas the Lime Crest occurrence is in coarse marble. The Greenland and Indian occurrences appear to be accidents of sedimentary geochemistry, but the New Jersey green micas almost certainly result at least in part from secondary fluid-related processes that formed the veins at Lime Crest.

There are no other published reports of Cr mineralization in the Grenville marbles, but Lea and Dill (1968) reported a significant association of barite with ore minerals in the Balmat-Edwards district in the northwestern Adirondacks. This is an important point because they described barite associated with massive anhydrite layers in Grenville marble, which were suggested to be evaporite horizons. Although there are no detailed descriptions of barite occurrences from Grenville marbles south of Balmat-Edwards, barite has been commonly reported among gangue minerals at Sterling Hill and Franklin (see Wilkerson, 1962, p. 14), and it seems likely that barite in chemical sediments interlayered with the Franklin Marble served as the source of Ba for vein-related metamor-

Table 3. Selected electron microprobe analyses of barian, zincian biotite and chlorian, zincian anandite from Sterling Hill skarn

	1	2	3	4	5	6	7	8	9	10	11	12
SiO_2	34.11	32.87	31.91	31.48	31.98	30.78	29.44	29.38	25.27	21.98	20.58	19.94
TiO_2	0.98	0.83	1.03	2.07	1.35	1.64	1.46	1.22	1.29	0.94	0.75	0.70
Al_2O_3	12.76	12.80	13.12	12.69	13.11	13.23	13.47	13.91	14.02	12.89	14.04	14.43
Cr_2O_3	0.03	0.07	0.06	0.05	0.06	0.07	0.08	0.06	0.09	0.12	0.12	0.11
FeO	13.13	14.46	16.48	15.63	14.02	15.00	19.03	17.58	20.45	24.24	24.96	25.89
MnO	1.77	2.12	2.36	2.36	1.87	2.29	1.50	1.39	1.91	2.32	2.30	2.40
MgO	12.24	10.37	8.79	7.61	11.24	8.52	8.30	9.60	5.56	2.61	2.15	1.80
ZnO	7.37	8.39	7.94	9.44	6.84	9.00	4.79	4.58	5.46	5.26	4.66	4.05
NiO	0.11	0.08	0.10	0.14	0.14	0.14	0.15	0.15	0.19	0.23	0.23	0.24
CaO	0.15	0.11	0.12	0.12	0.12	0.13	0.10	0.13	0.13	0.20	0.46	0.38
BaO	6.26	6.97	7.63	7.95	8.65	9.22	12.57	13.65	18.45	21.87	22.40	23.05
Na_2O	0.18	0.07	0.11	0.19	0.20	0.20	0.09	0.14	0.17	0.14	0.16	0.08
K_2O	7.14	6.83	6.53	6.38	6.20	5.82	4.55	4.25	2.28	0.81	0.52	0.36
F	1.62	1.48	1.05	1.05	2.88	1.78	1.17	1.49	0.99	0.50	0.66	0.83
Cl	0.89	1.01	1.20	1.25	1.20	1.12	2.22	1.30	2.99	6.16	6.96	7.15
Total	98.74	98.46	98.43	98.41	99.86	98.94	98.92	99.42	99.25	100.27	100.95	101.41
$-O = F$	0.68	0.62	0.44	0.44	1.21	0.75	0.49	0.63	0.42	0.21	0.28	0.35
$-O = Cl$	0.20	0.22	0.26	0.28	0.26	0.25	0.49	0.29	0.66	1.36	1.53	1.57
Total	97.86	97.62	97.73	97.69	98.39	97.94	97.94	98.50	98.17	98.70	99.14	99.49
Formulas calculated on 11 O atom anhydrous basis												
Si	2.761	2.725	2.681	2.672	2.662	2.622	2.564	2.537	2.364	2.237	2.120	2.070
Al	1.217	1.250	1.300	1.269	1.287	1.328	1.383	1.417	1.546	1.547	1.706	1.765
Fe^{2+}	0.022	0.025	0.019	0.059	0.051	0.050	0.053	0.046	0.090	0.216	0.174	0.165
	4.000	4.000	4.000	4.000	4.000	4.000	4.000	4.000	4.000	4.000	4.000	4.000
Ti	0.060	0.052	0.065	0.132	0.085	0.105	0.096	0.079	0.091	0.072	0.058	0.054
Cr	0.002	0.004	0.004	0.003	0.004	0.005	0.006	0.004	0.006	0.009	0.010	0.009
Fe^{2+}	0.867	0.978	1.139	1.050	0.925	1.018	1.333	1.225	1.510	1.847	1.977	2.082
Mn	0.122	0.149	0.168	0.170	0.132	0.165	0.111	0.102	0.151	0.200	0.200	0.211
Mg	1.476	1.281	1.101	0.963	1.395	1.082	1.078	1.236	0.776	0.396	0.331	0.278
Zn	0.440	0.513	0.512	0.591	0.420	0.556	0.308	0.292	0.377	0.395	0.355	0.311
Ni	0.007	0.006	0.007	0.009	0.009	0.010	0.011	0.011	0.014	0.019	0.019	0.020
	2.974	2.983	2.996	2.918	2.970	2.951	2.943	2.949	2.925	2.938	2.950	2.965
Ca	0.013	0.009	0.011	0.011	0.011	0.012	0.009	0.012	0.013	0.022	0.051	0.042
Ba	0.198	0.226	0.251	0.264	0.282	0.308	0.429	0.462	0.676	0.872	0.904	0.938
Na	0.028	0.011	0.018	0.031	0.032	0.032	0.016	0.023	0.031	0.027	0.032	0.017
K	0.737	0.723	0.700	0.691	0.659	0.633	0.505	0.469	0.273	0.105	0.068	0.047
	0.976	0.969	0.980	0.997	0.984	0.985	0.959	0.966	0.963	1.026	1.055	1.044
F	0.415	0.389	0.278	0.282	0.759	0.478	0.322	0.407	0.293	0.159	0.217	0.272
Cl	0.123	0.142	0.171	0.180	0.170	0.162	0.328	0.193	0.474	1.063	1.216	1.258
	0.538	0.531	0.449	0.462	0.929	0.640	0.650	0.600	0.767	1.222	1.433	1.530

phic micas. Barium feldspars have been reported as common in silicate skarns from the Franklin mine and as occurring at Sterling Hill (Frondel et al., 1966). No obvious source for Cr can be located in the vicinity of the Franklin Marble, and chromite-bearing ultramafic rocks are notably rare in the Grenville.

Presumably both Ba and Cr were mobilized from their sources and transported into the marble at Lime Crest by metamorphic solutions that participated in the formation of the green micas. The zoning of the larger muscovite crystals in the veins suggests that the vein fluids evolved in their Ba, Na, and Cr contents from higher to lower during muscovite growth. High F contents of the fluorian phlogopite and the sporadic presence of fluorite in the veins argue for high f_{HF} and f_{F_2} in the vein fluids. Valley et al. (1982) calculated fugacities at 650 °C and 6 kbar for these species in Adirondack marbles containing F-rich phlogopite and F-rich tremolite in the ranges of $\log f_{HF} = -1.27$ to -0.37 and $\log f_{F_2} = -34.19$ to -33.43.

Barian biotite at Sterling Hill

Petrography and mineral chemistry

Interspersed with the famous willemite-zincite-franklinite zinc ores of Franklin and Sterling Hill are non-ore zinc-bearing calc-silicate and skarn zones. Specimen SU-202 was sampled from one of these skarns as part of a New Jersey Zinc Co. diamond drill core and was first studied in detail by Reilly (1983). She described the assemblage in SU-202 as zincian clinopyroxene (greater than 90% modally) with minor willemite, sphalerite, gahnite, calcite, and barian biotite. The biotite forms small (several hundred micrometers), rounded grains with distinctive orange-brown color in plane light and moderate birefringence. Microprobe analyses indicate that individual grains are not chemically zoned, but the variation in composition from grain to grain is significant and the darker colored grains appear to be richest in Ba and Fe. No systematic pattern of distribution of Ba-rich and Ba-poor biotite grains has been discerned within the thin section, and it is therefore impossible to distinguish texturally the earlier and later formed grains.

Microprobe analyses showing the range of compositions of barian biotite are given in Table 3. All of the analyses reported in the table were completed on different grains in a single probe section. Strictly speaking, the most Ba-rich of these minerals are properly called anandite, since greater than two-thirds of the interlayer cations are Ba and their Fe/Mg ratios are high (Table 3, analyses 10–

12). Anandite as defined (Pattiaratchi et al., 1967; Guggenheim, 1984) is an Fe- and Ba-rich brittle mica that is characteristically found in skarns. The other previously reported types of barian biotite, barian phlogopite and kinoshitalite, are compositionally quite different from the Sterling Hill barian biotite and occur in marbles or calc-silicates rather than skarns. The several compositional distinctions between the present micas and previously described barian biotite include the presence of substantial contents of Mn, Zn, and Cl in the Sterling Hill micas and the absence in them of S, which is typical of anandite. Zn and Cl contents appear to be uniquely high, but Mn contents are less than those of barian phlogopite from Långban (Frondel and Ito, 1968). In fact, the high Cl content of the anandite from Sterling Hill (up to 1.0–1.2 Cl per 12 anion formula) makes them 50–60% of the chlorian end-member and may qualify the most Cl-rich as a new species.

An explanation is in order regarding the reporting of structural formulas in Table 3. Previous reports of anandite have indicated a systematic deficiency of (Si + Al) from 4.0 per 11 O atoms. Guggenheim (1984) noted that the substantial tetrahedral site deficiency seems to be made up by Fe (either Fe^{3+} or Fe^{2+}), citing X-ray scattering factors. Because of the typical preference of Zn for tetrahedrally coordinated sites in minerals, it may be possible that some or much of the Zn occurs in the tetrahedral sites in this mica. However, because $^{[4]}Fe$ has been documented in anandite, this protocol has been used in Table 3. In their paper on the zincian mica hendricksite, Frondel and Ito (1966) reported structural formulas showing Zn as solely octahedral. On the other hand, Dunn et al. (1984) have reported $^{[4]}Zn$ in minehillite, and Peacor et al. (1988) have also reported it in franklinfurnaceite, a layer silicate from Franklin. Obviously, anandite from other localities likely has insufficient Zn to make up any tetrahedral deficiency, but there is more than enough Zn in the Sterling Hill micas, and further X-ray site study of this mineral is warranted.

The obviously high total cation sums in the formulas for analyses 10–12, particularly for the interlayer cations, suggest that too many cations have been calculated for 11 anions and that a significant fraction of the Fe is therefore Fe^{3+}. As an example, assuming that Ca, Na, Ba, or K cannot go into any other site, analysis 11 could be normalized to some reasonable arbitrary sum of interlayer cations, say 0.98, reflecting the typical nearly complete A site in trioctahedral micas. If this is done, the recalculated formula is deficient in the O required to make up the basic sheet silicate structure, i.e., 10.0 O atoms. Adding the requisite number of O atoms per formula unit requires conversion of about 35% of the Fe^{2+} to Fe^{3+}. This recalculation scheme would create more than enough Fe^{3+} to fill the roughly 0.5-cation deficiency in the tetrahedral sites, but because it is arbitrary, it has not been done for the analyses in Table 3. It is clear, however, that the formulas in Table 3 qualitatively indicate the presence of sufficient Fe^{3+} to fill the tetrahedral sites.

As was done above for the Lime Crest muscovite, a

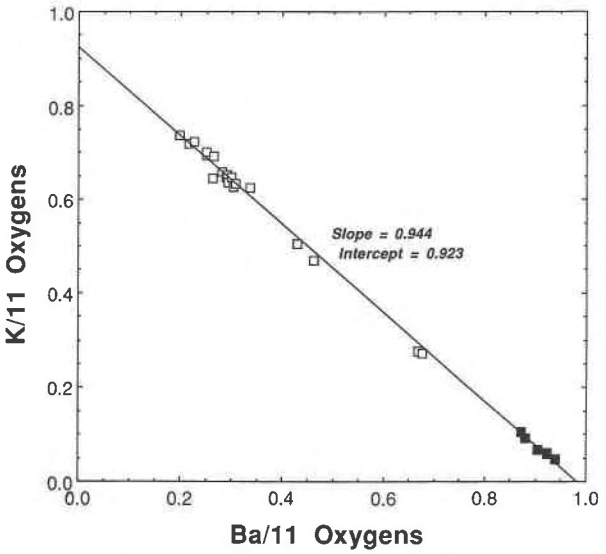

Fig. 6. Correlation of Ba and K in Sterling Hill barian micas. In this and succeeding plots, the data are separated into two groups: analyses with >0.70 Ba/11 O atoms (filled squares) and analyses with <0.70 Ba (open squares). The division was chosen to separate the data into two sets with the most consistent behavior. The least-squares line was fitted to all the data, and its slope of 0.944 indicates virtually no involvement of other alkalis or alkaline earths in the A site, with the exception that the slope of slightly less than 1.0 reflects minor enrichment of Ca in the A site of the high-Ba biotite (see formulas in Table 3).

series of exchange components can be constructed for the Sterling Hill barian biotite that, along with the additive component phlogopite, $KMg_3AlSi_3O_{10}(OH)_2$, completely describes barian biotite composition space algebraically. These exchange components, or exchange vectors, include (classified by type of size) interlayer (coupled with tetrahedral): (1) $BaAlK_{-1}Si_{-1}$, (2) $BaFe^{3+}K_{-1}Si_{-1}$, (3) NaK_{-1}, (4) $CaAlK_{-1}Si_{-1}$; octahedral: (5) $R^{2+}Mg_{-1}$ (for Fe, Zn, Mn, Ni), (6) $TiAl_2Mg_{-1}Si_{-2}$ (Ti-Tschermak), (7) $R^{3+}_2[\ ]Mg_{-3}$ (for Fe or Cr), (8) $R^{2+}_2Mg_{-1}Si_{-1}$ (generalized Tschermak); tetrahedral: (9) $Fe^{3+}Al_{-1}$; and O_3 anion: (10) $Cl(OH)_{-1}$, (11) $F(OH)_{-1}$.

There is significant sympathetic variation of a number of chemical components with Ba. First, and fairly obviously, there is complementary decrease in K in the interlayer sites as Ba increases (Fig. 3) (exchange component 1). Note that the Na content of the interlayer site remains constant at about 2–3%, in contrast to the high Na content of the barian, fluorian phlogopite from Lime Crest (up to 25%). The diadochy of Ba and K is emphasized in Figure 6, but the very slight negative deviation from a slope of 1.0 suggests systematically slightly higher Na contents in the Ba-rich micas.

The phases richer in Ba are brittle micas, and therefore there should be a positive correlation between (Ba + Ca) and $^{[4]}Al$ (exchange components 1 and 3), as shown in Figure 7. This figure is the first of several that show different patterns of chemical behavior for the micas with Ba > 0.65 (shown as filled squares on the plots) from

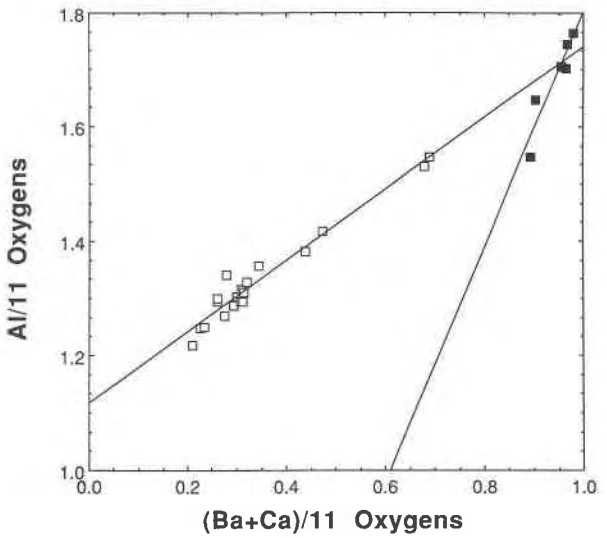

Fig. 7. Correlation of (Ba + Ca) and Al_{tot} in the Sterling Hill barium biotite. See Figure 6 caption for explanation of symbols.

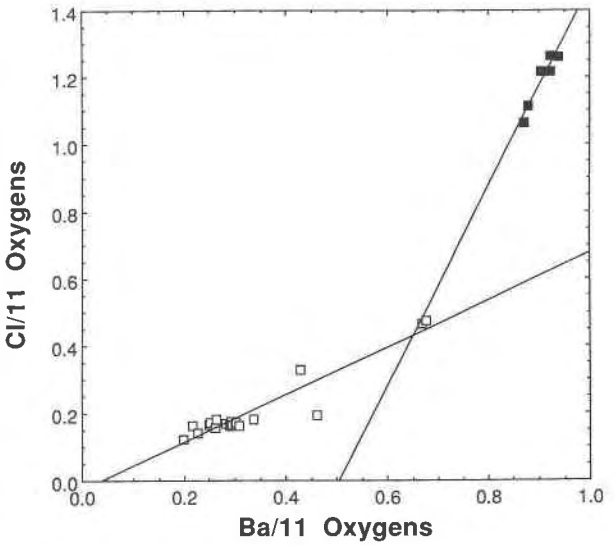

Fig. 8. Correlation of Ba and Cl for Sterling Hill barian micas. See Figure 6 caption for explanation of symbols. Both sets of data have been fitted with least-squares fits, but a logarithmic function through both sets of data gives an equally good fit.

those with Ba < 0.65 (shown as open squares). There is no distinction between high- and low-Ba micas in Figure 6, but Figure 7 clearly shows that coupled Ba-Al substitutions in the highest Ba biotite are different from those in the low- to intermediate-Ba biotite. These data suggest that for biotite with less than 0.65 Ba/11 O atoms, Ba substitution is largely, but not entirely, accommodated by exchange component 1. The slope of the least-squares line through the low-Ba data is considerably less than 1.0 (about 0.75), indicating a major extent of an additional coupled interlayer-tetrahedral exchange, probably component 2. At higher Ba contents the exchange mechanism changes significantly. Close examination shows that a mica with Ba content of 0.90/11 O atoms has the same total Al content as mica with 0.65 Ba/11 O atoms. This suggests substantially greater operation of exchange 2 in the high-Ba group than in the other group. However, the large slope of the line through the high-Ba data (about 2.0) also indicates $^{[4]}$Al in excess of that required by sole operation of exchange 1 and suggests that one or more Tschermak's substitutions operate more in these micas than in the low-Ba ones.

The discrepant behavior of high- and low-Ba micas is also apparent in Figure 8, a plot of Ba vs. Cl. Cl increases linearly from about 0.12/11 O atoms at low Ba up to 0.5 at a Ba content of 0.65. Micas with Ba content over 0.9/11 O atoms, however, have Cl in excess of 1.0. I have not found any reports in the literature of other similarly Cl-rich micas. It is interesting that the most Cl-rich mica grains have the highest Fe contents and are the richest in Ba (Fig. 9). There is also a strong negative correlation between Ba and F and between Fe and F. These latter effects are in accord with the well-known crystal chemical behaviors of Mg-Cl and Fe-F avoidance (Valley et al., 1982).

Correlation of Ba content with concentrations of various measured transition metals is more problematic. Figure 9 shows generally good positive correlation between Ba and either Fe, Ni or Mn, although in the Ba-Mn plot the increase of Mn is inconsistent between the low-Ba and high-Ba data sets. On the other hand, there is more chaotic behavior in the Ba-Zn and Ba-Ti plots. Within the low-Ba data on both plots, there does not appear to be any particular correlation. Both Zn and Ti are similar, however, in having lower concentrations in the high-Ba micas than in the low-Ba ones, a behavior unlike the other elements considered.

The subtle variability of Mn and pronounced variability of Zn and Ti in the low-Ba biotite argue for more complex fractionation patterns for these elements between matrix and biotite in the low-Ba group than in the high-Ba group. If one accepts that the high-Ba micas crystallized earliest and were succeeded by the low-Ba ones (as suggested below), then the behavior of the trace components Cl, Fe, and Ni is as expected for major depletion of trace components from a reservoir, and behavior of major components (in this unusual bulk composition!) Mn and Zn show more complex intercrystalline fractionations. In this regard, the behavior of Ti is unexpected because it should behave as a trace constituent and not as a major one.

Origin of barian biotite and chlorian anandite at Sterling Hill

Although it is possible that the apparent elemental correlations are merely accidents of crystallization, it is more satisfying to presume that the fractionations result either from chemical evolution of the rock reservoir during mica formation or from systematic compatibility-incompatibility relationships. Recent research by Johnson (1990)

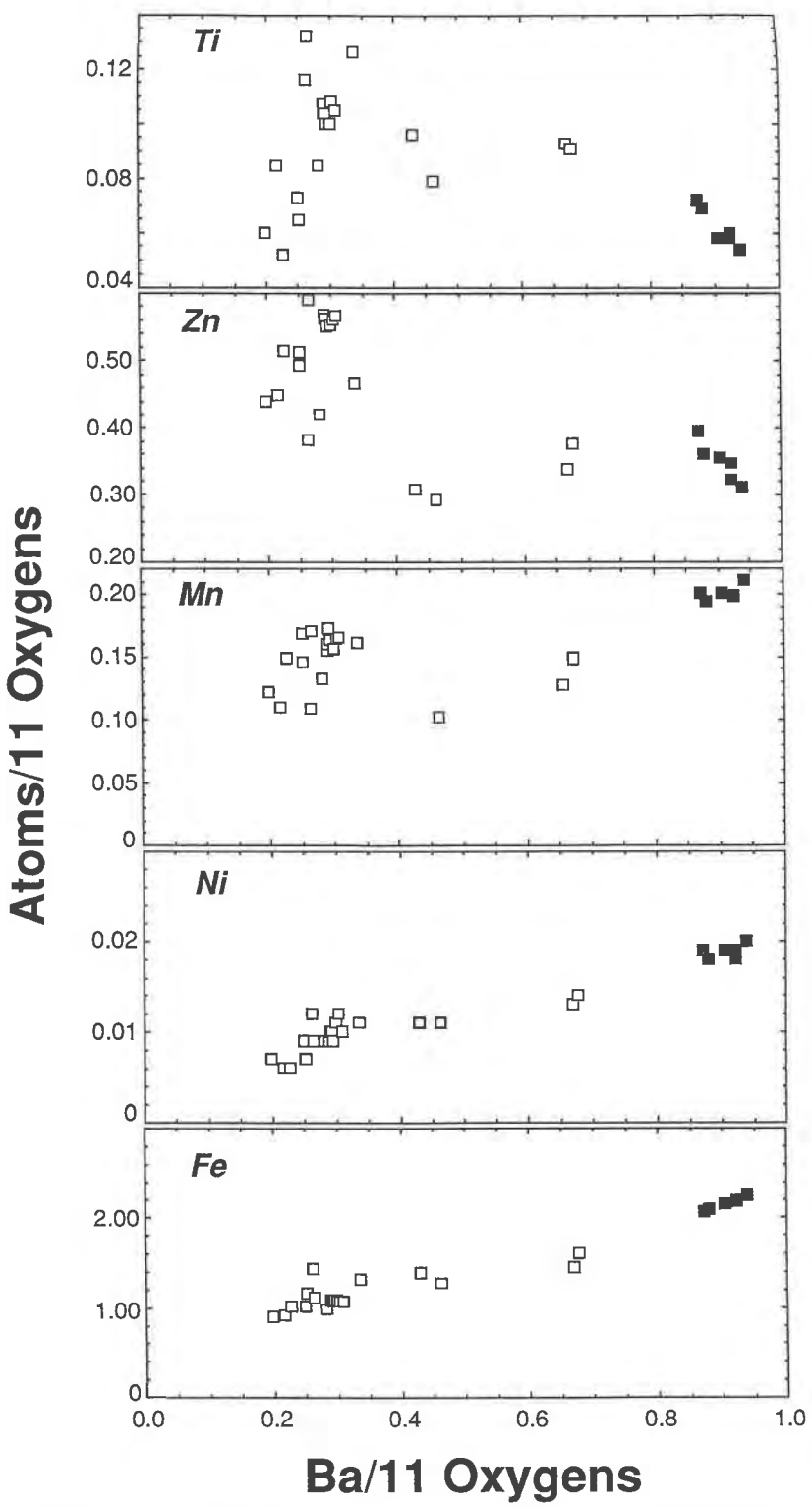

Fig. 9. Correlation of Ba with contents of each of five metals (Fe, Ni, Mn, Zn, and Ti) in Sterling Hill barian micas. See Figure 6 caption for explanation of symbols. Note that for both Fe and Ni, there is a good linear correlation with Ba for all analyses, whereas for Mn the correlation is better for the high-Ba group than for the low-Ba group. For Zn and Ti, there seem to be good correlations only within the highest-Ba group.

on the origin of the Sterling Hill deposit has produced evidence that the protolith for both ores and skarns was not a sea-floor massive sulfide like Balmat-Edwards but rather a hot-chemical brine deposit comprising oxides, hydroxides, and hydroxysilicates of Mn and Zn, similar to deposits that are presumed to be forming now from hot brine pools on the Red Sea floor.

As noted in the introduction, sedimentary or hydrothermal barite is the most probable source for the Ba that was incorporated in the micas at Sterling Hill. Johnson (1990) does not discuss barite in his model for the deposit, but it may well have been a part of the hydrothermal ore deposition event. High solubility of barium sulfide in hot brines under reducing transport conditions, coupled with low solubility of barium sulfate under oxiding conditions when the hot brines came in contact with sea water, could have resulted in precipitation of at least minor barite in the ore protolith. Complex precipitation or diagenetic reactions may even have produced barian feldspars or other barian minerals.

Regardless of how the protolith formed, it is obvious that the present mineral assemblages of both ores and non-ores at Sterling Hill (including the barian micas) are a result of the granulite-grade Grenville metamorphism in the Proterozoic. A confident assessment of the chemical evolution of barian mica formation requires more paragenetic evidence than we have regarding whether low- or high-Ba micas came first. We can, however, construct a reasonable scenario. If we presume that the protolith for the skarn had an admixed minor barite component, perhaps stirred in tectonically in the early deformation of the deposit, it is reasonable to suppose that the barite would have been rendered unstable at a relatively early stage of the metamorphic heating: sulfate minerals are virtually unknown in high-grade metamorphic rocks.

Reduction or decomposition of the sulfate in a metamorphic environment consisting of Mn- and Zn-rich ore minerals, residual pore fluids, and perhaps a minor detrital sedimentary component might be expected to have produced a Ba-rich sheet silicate that was either a precursor phase to the barian mica or the mica itself. Crystallization of a small amount of Cl-rich mica would have significantly depleted the Cl in the pore fluid reservoir. If the skarn protolith had a small initial barite component, formation of the early Ba-rich sheet silicate would also have depleted the Ba reservoir and resulted in later formation of progressively Ba-poorer micas. In this scenario, the sphalerite in the skarns might well have been produced by reduction of sulfate accompanying the breakdown of barite, with resultant sulfidation of zinc minerals to form sphalerite. O produced in this process may help to explain the mysterious apparent oxidation event, noted by Johnson (1990), that resulted in the bleaching and total graphite removal from marble horizons in the ore deposit and periphery.

The concentrations of minor elements such as Fe, Ni, and Mn mimic the behavior of Ba closely (Fig. 9), suggesting that they also were more compatible in the newly formed sheet silicate and were simply partitioned from the reservoir into the micas. However, the fractionation behavior of Mn becomes more complicated at a late stage in mica formation. On the other hand, Zn is more highly concentrated in the Ba-poor micas (Fig. 9). The major Zn reservoir in the local metamorphic assemblage is zincian augite, which contains about 5 wt% ZnO and constitutes about 90% of the rock. Gahnite and sphalerite, although present, occur in very small amounts and are embayed and corroded. This texture suggests breakdown of these Zn-rich phases at peak metamorphic conditions, accompanied by progressive enrichment of the Ba-poor mica in Zn. Ti shows the most complicated behavior. Apparent enrichment of Ti from low concentrations in Ba-rich micas to higher values in intermediate micas is succeeded by wildly variable Ti contents of the most Ba-poor micas. These data may reflect highly localized Ti enrichment at a late stage resulting from limited Ti mobility in the rock.

Summary

The unusual micas described in this paper add to the long list of compositionally remarkable minerals that have been found in the Franklin Marble. The complexity of petrologic phenomena that characterize the marble is emphasized by the fact that the barian micas from the Lime Crest quarry show such diverse compositional behavior. Similarly, the enormous range in barian mica compositions within a single skarn sample from the Sterling Hill ore deposit underlines the genetic complexity for ore- and skarn-forming processes.

Barian, chromian muscovite and barian, fluorian phlogopite from Lime Crest have been found associated with albite-fluorite-rutile veins in coarse calcite-dolomite marble. Barian micas appear to be restricted to the veins, strongly supporting a vein-fluid involvement in the formation of these micas. The presence of fluorite demonstrates that the vein fluids were at fluorite saturation under the local conditions. Conspicuously lower F contents for muscovite than for phlogopite indicate that the solubility of F in the two phases varied significantly under conditions of probable fluorite saturation. Chemical zoning of larger muscovite grains, with core-to-rim decreases in Ba, Na, and Cr, suggests chemical evolution of vein fluid chemistry as mica crystallized. Interaction of marble with vein fluids was remarkably minor, inasmuch as the veins contain essentially pure albite and the muscovite has very little Ca.

On the other hand, formation of barian biotite and chlorian anandite in skarn at Sterling Hill can be visualized as an approximately isochemical metamorphic process without involvement of externally derived fluids. The most likely source of Ba for these volumetrically minor phases was a small amount of barite admixed with hydrothermally derived ore and skarn protoliths. A small component of detrital material is also required to provide silica, alkalis, and Fe. During heating of the protoliths the sulfate could have been reduced to sulfide at roughly constant f_{O_2}, and product minerals would have included Ba-

bearing sheet silicates and sphalerite. The most Ba-rich and Cl-rich micas probably formed earliest, and successive formation of barium biotite tapped progressively depleted local reservoirs of Ba and Cl.

Fractionation of metal ions into the micas was determined by the nature of the assemblage and the stability and compositional evolution of constituent minerals during metamorphism. Fe^{2+} is generally in short supply in both ore and non-ore assemblages from the deposit (Johnson, 1990), but it occurs in significant concentrations in the early, Ba-rich micas. Mn and Ni behave similarly to Fe: they would have been depleted early from the reservoir, and the later crystallized micas therefore grew progressively poorer in these metals. Zn and Ti, however, appear to have become enriched in the rock as biotite grew, because the late, Ba-poor biotite is enriched in these elements.

Acknowledgments

The author is particularly appreciative of the excellent research effort by Laura K. Reilly, who first identified the Ba-rich sheet silicate in the Sterling Hill skarn. I also thank Bob Freas, the chief geologist for the Limestone Products Corporation quarry at Lime Crest in 1983, who allowed us access to the quarry, and R.J. Metsger, the chief geologist for New Jersey Zinc Corporation's Sterling Hill mine. Todd N. Solberg was of great help in doing difficult probe analyses in the Microprobe Laboratory, VPI and SU. The manuscript was much improved by the reviews of James Post, Richard Wendlandt, and particularly Pete Dunn. The National Science Foundation provided financial support for this work through grant EAR 84-17445 (to B.J. Skinner, R.J.T., and D.M. Rye, Yale University).

References cited

Bauer, L.H., and Berman, H. (1933) Barium muscovite from Franklin, N.J. American Mineralogist, 18, 30.

Bol, L.C.G.M., Bos, A., Sauter, P.C.C., and Jansen, J.B.H. (1989) Barium-titanium-rich phlogopites in marbles from Rogaland, southwest Norway. American Mineralogist, 74, 439–447.

Carvalho, A.V., III, and Sclar, C.B. (1988) Experimental determination of the $ZnFe_2O_4$-$ZnAl_2O_4$ miscibility gap with application to franklinite-gahnite exsolution intergrowths from the Sterling Hill zinc deposit, New Jersey. Economic Geology, 83, 1447–1452.

Devaraju, T.C., and Anantha, M.K.D. (1978) Mineralogy of the fuchsites from Gattihosahalli, Chiradurga District. Proceedings of the Indian Academy of Science, 87, 255–261.

Dunn, P.J. (1984) Barian muscovite from Franklin, New Jersey. Mineralogical Magazine, 48, 562–563.

Dunn, P.J., Peacor, D.R., Leavens, P.B., and Wicks, F.J. (1984) Minehillite, a new layer silicate from Franklin, New Jersey, related to reyerite and truscottite. American Mineralogist, 69, 1150–1155.

Dymek, R.F., Boak, J.L., and Kerr, M.T. (1983) Green micas in the Archean Isua and Malene supracrustal rocks, southern West Greenland, and the occurrence of a barian-chromian muscovite. Rapport Grønlands Geoliske Undersoegelse, 112, 71–82.

Frondel, C., and Baum, J.L. (1974) Structure and mineralogy of the Franklin zinc-iron-manganese deposit, New Jersey. Economic Geology, 69, 157–180.

Frondel, C., and Ito, J. (1966) Hendricksite, a new species of mica. American Mineralogist, 51, 1107–1123.

——— (1968) Barium-rich phlogopite from Långban, Sweden. Arkiv Mineralogie Geologie, 4, 445–447.

Frondel, C., Ito, J., and Hendricks, J.G. (1966) Barium feldspars from Franklin, New Jersey. American Mineralogist, 51, 1388–1393.

Gaspar, J.C., and Wyllie, P.J. (1982) Barium phlogopite from the Jacupiranga carbonatite, Brazil. American Mineralogist, 67, 997–1000.

Guggenheim, S. (1984) The brittle micas. In Mineralogical Society of America Reviews in Mineralogy, 13, 61–104.

Heinrich, K.F.J. (1981) Electron beam X-ray microanalysis, 578 p. Van Nostrand, Reinhold and Co., New York.

Johnson, C.A. (1990) Petrologic and stable isotopic studies of the metamorphosed zinc-iron-manganese deposit at Sterling Hill, New Jersey, 108 p. Ph.D. thesis, Yale University, New Haven, Connecticut.

Lea, E.R., and Dill, D.B., Jr. (1968) Zinc deposits of the Balmat-Edwards District, New York. In J.D. Ridge, Ed., Ore deposits of the United States, 1933–1967, p. 20–48. AIME, New York.

Mansker, W.L., Ewing, R.C., and Keil, K. (1979) Barian-titanian biotites in nephelinites from Oahu, Hawaii. American Mineralogist, 64, 156–159.

Pattiaratchi, D.B., Saari, E., and Sahama, Th.G. (1967) Anandite, a new barium iron silicate from Wilagedera, Northwestern Province, Ceylon. Mineralogical Magazine, 36, 1–4.

Peacor, D.R., Rouse, R.C., and Bailey, S.W. (1988) Crystal structure of franklinfurnaceite: A di-trioctahedral zincosilicate intermediate between chlorite and mica. American Mineralogist, 73, 876–887.

Reilly, L.K. (1983) An analysis of calc-silicate bands of the Sterling Hill zinc deposit, Sussex County, New Jersey, 90 p. B.S. thesis, Yale University, New Haven, Connecticut.

Solie, D.N., and Su, Shu-Chun (1987) An occurrence of Ba-rich micas from the Alaska Range. American Mineralogist, 72, 995–999.

Valley, J.W., Peterson, E.U., Essene, E.J., and Bowman, J.R. (1982) Fluorphlogopite and fluortremolite in Adirondack marbles and calculated C-O-H-F fluid composition. American Mineralogist, 67, 545–557.

Wendlandt, R.F. (1977) Barium-phlogopite from Haystack Butte, Highwood Mountains, Montana. Carnegie Institution of Washington Year Book, 76, 534–539.

Wilkerson, A.S. (1962) The minerals of Franklin and Sterling Hill, New Jersey. Bulletin 65, New Jersey Geological Survey, Department of Conservation and Economic Department, Trenton, New Jersey.

Yoshii, M., Maeda, K., Kato, T., Watanabe, T., Yui, S., Kato, A., and Nagashima, K. (1973) Kinoshitalite, a new mineral from the Noda-Tamagawa mine, Iwate Prefecture. Chigaku Kenkyu, 24, 181–190 (not seen; abstracted in American Mineralogist, 60, 486–487, 1975).

Manuscript received March 19, 1990
Manuscript accepted May 23, 1991